

ESTIMATING PROBABILITIES OF MULTIVARIATE FAILURE SETS BASED ON PAIRWISE TAIL DEPENDENCE COEFFICIENTS

BY ANNA KIRILIOUK^{1,a} AND CHEN ZHOU^{2,b}

¹Namur Institute for Complex Systems (Naxys), Université de Namur, Belgium, ^aanna.kiriliouk@unamur.be

²Econometric Institute, Erasmus University Rotterdam, ^bzhou@ese.eur.nl

An important problem in extreme-value theory is the estimation of the probability that a high-dimensional random vector falls into a given extreme failure set. This paper provides a parametric approach to this problem, based on a generalization of the tail pairwise dependence matrix (TPDM). The TPDM gives a partial summary of tail dependence for all pairs of components of the random vector. We propose an algorithm to obtain an approximate completely positive decomposition of the TPDM. The decomposition is easy to compute and applicable to moderate to high dimensions. Based on the decomposition, we obtain parameters estimates of a max-linear model whose TPDM is equal to that of original random vector. We apply the proposed decomposition algorithm to industry portfolio returns and maximal wind speeds to illustrate its applicability.

1. Introduction. Extreme value statistics deal with the characterization of extreme events, such as stock market crashes, that occur with low frequency but with a potentially severe impact. A typical extreme value question is to estimate the (low) probability of such an extreme event. In the context of multivariate extremes, we are interested in estimating the probability that a d -dimensional random vector $\mathbf{X} = (X_1, \dots, X_d)$ falls into some “extreme region” C (also called failure region). For example, in the example of portfolio risk, the components of \mathbf{X} represent negative log-returns of d stocks in a portfolio. Another example is in catastrophic climate events, where \mathbf{X} may represent maximum daily rainfall amounts at d monitoring stations. To estimate such a probability $\mathbb{P}[\mathbf{X} \in C]$, it is important to take the tail dependence across the margins of \mathbf{X} into account, i.e., the tendency of extremes to occur in several components simultaneously.

In practice, the extreme region of interest might contain few or even no observed data points, especially when the dimension d is large. One potential solution is to employ appropriate parametric models for multivariate extremes and to estimate the model parameters using intermediate level observations. However, as the dimension of the vector \mathbf{X} increases, such a parametric approach becomes increasingly complex, which leads to the following dilemma. On the one hand, models with a small number of parameters tend to oversimplify the tail dependence structure. On the other hand, models with many parameters are difficult to estimate and may even lead to overfitting.

This paper provides a parametric model for the case where the underlying random vector is high dimensional. The model can capture the so-called tail dependence coefficients for all pairs of components of the d -dimensional random vector. Even though it has a large number of parameters (up to $d(d+1)/2$), they are easily obtained based on a fast algorithm, allowing one to approximate the failure probability using the estimated model. Other estimators of (multivariate) failure probabilities are proposed in [Drees and de Haan \(2015\)](#) (for the bivariate case) and [Valk \(2016\)](#), among others.

In the existing literature, tail dependence of \mathbf{X} is characterized in various ways, such as by the exponent measure, the angular measure, and the stable tail dependence function,

Keywords and phrases: Extreme-value theory, Tail dependence, Max-linear model.

among others (Beirlant et al., 2004; de Haan and Ferreira, 2006). While such objects fully characterize the extremal behavior of a random vector, their estimation in high dimensions suffers from the “curse of dimensionality”. Instead, one may consider a partial summary of tail dependence by focusing on the tail dependence coefficients χ or the extremal coefficients θ for all pairs, see e.g. Coles, Heffernan and Tawn (1999). This is similar to summarizing the dependence structure of a random vector by the covariance or correlation matrix.

In this paper, we focus on a generalization of the so-called *tail pairwise dependence matrix* (TPDM), which collects all pairwise tail dependence coefficients. This dependence matrix was originally proposed by Larsson and Resnick (2012) and has gained in popularity since the work of Cooley and Thibaud (2019); for example, Klüppelberg and Krali (2021) use it to estimate the parameters of an extreme Bayesian network, Fomichov and Ivanovs (2020) propose a clustering algorithm inspired by spherical k -means, where the means are replaced by the Perron–Frobenius eigenvectors of the TPDM, and Kim and Kokoszka (2022) study the extremal dependence between vectors of scores of functional data.

The TPDM is particularly appropriate when \mathbf{X} is multivariate regularly varying with tail index $\alpha = 2$. By contrast, our approach allows for multivariate regular variation with a general tail index α , without standardizing the data to $\alpha = 2$. Since marginal standardization does not affect dependence modeling, it is common in practice to separate marginal and dependence modeling by first estimating the marginal distributions (parametrically or non-parametrically), standardizing each marginal to a common distribution, and then modeling the dependence structure only. However, such an approach can be suboptimal in some applications. For example, in the portfolio risk example, if one intends to estimate the Value-at-Risk or the Expected Shortfall of a portfolio loss $L = \sum_{j=1}^d v_j X_j$, where v_1, \dots, v_d represent weights of the stocks (see, e.g., Mainik and Embrechts, 2013), the failure region is of the form $\{\sum_j v_j X_j > x\}$ with x large. In this case, we need to directly model the original vector \mathbf{X} : a nonparametric transformation for the marginals will lead to untractable failure regions. Our approach without standardizing a priori is therefore necessary. Such failure regions are also of interest in climate applications, where $\sum_{j=1}^d v_j X_j$ represents the spatial average over a given region of some environmental variable (see, e.g. Kiriliouk and Naveau, 2020).

The tail pairwise dependence matrix is closely related to the max-linear model, a simple but rather flexible multivariate extreme-value model. In such a model, each component of a d -dimensional vector can be interpreted as the maximum shock among a set of q independent heavy-tailed factors. The max-linear model has $d \times q$ parameters (or $d \times (q - 1)$ when margins are standardized), usually stocked in a parameter matrix $A \in \mathbb{R}^{d \times q}$. Max-linear models are, among other applications, used to model extremes on directed acyclic graphs (Gissibl and Klüppelberg, 2018) or latent factor structures for financial returns (Cui and Zhang, 2018). If the number of parameters is limited, one can use the minimum distance estimation (Einmahl, Kiriliouk and Segers, 2018) or spherical k -means (Janßen and Wan, 2020) to estimate a max-linear model. Kiriliouk (2020) presents hypothesis tests aiding in deciding the size of q .

Theoretically, Fougères, Mercadier and Nolan (2013) showed that the max-linear model is dense in the class of d -dimensional multivariate extreme-value distributions. Moreover, Cooley and Thibaud (2019) showed that there exists a finite $q \in \mathbb{N}$ such that the tail pairwise dependence matrix $\Sigma_{\mathbf{X}}$ of any multivariate regularly varying random vector \mathbf{X} with $\alpha = 2$ is equal to that of a max-linear model with q factors via the relation $\Sigma_{\mathbf{X}} = AA^T$. In practice, the parameter matrix A of this max-linear model can be estimated through a completely positive decomposition of $\Sigma_{\mathbf{X}}$. A matrix S is called *completely positive* if there exists a non-negative matrix A such that $S = AA^T$; finding this matrix A amounts to finding a *completely positive decomposition* of S . Positive decompositions are well studied in the linear algebra literature (Groetzner and Dür, 2020; Boj and Nguyen, 2021), where it is shown that the maximum

number of columns of A is $d(d+1)/2 - 4$. The positive decomposition can be obtained via a decomposition algorithm, nevertheless, the algorithm is computationally intensive.

In this paper, we propose an algorithm for an *approximate* completely positive decomposition $\Sigma_{\mathbf{X}} \approx AA^T$ with $A \in \mathbb{R}^{d \times d}$. The decomposition is easy to compute and applicable to moderate to high dimensions. In addition, it is fast enough to obtain various decompositions corresponding to a single TPDM and hence to characterize the model uncertainty. We show that the decomposition is exact when \mathbf{X} follows a max-linear model with a triangular coefficient matrix A . Moreover, in all other cases, the decomposition is exact for all off-diagonal entries of $\Sigma_{\mathbf{X}}$, but may overestimate its diagonal entries. We apply the proposed decomposition algorithm to industry portfolio returns and maximal wind speeds to illustrate its applicability. A third application, concerning rainfall in Switzerland, has been deferred to Appendix B.

2. Background.

2.1. *Multivariate regular variation and the tail pairwise dependence matrix.* Let $\mathbf{X} \in [0, \infty)^d$ be a random vector with joint cumulative distribution function F and continuous marginal distributions F_1, \dots, F_d . Write $\mathbb{E}_0 = [0, \infty]^d \setminus \{\mathbf{0}\}$. We assume that \mathbf{X} is *multivariate regularly varying*, i.e., there exists a sequence $b_n \rightarrow \infty$ and a limit measure $\nu_{\mathbf{X}}$ such that

$$(1) \quad n \mathbb{P} [b_n^{-1} \mathbf{X} \in \cdot] \xrightarrow{v} \nu_{\mathbf{X}}(\cdot), \quad \text{as } n \rightarrow \infty,$$

where \xrightarrow{v} denotes vague convergence in the space of non-negative Radon measures on \mathbb{E}_0 and $\nu_{\mathbf{X}}$ is called the *exponent measure* (Resnick, 2007, Chapter 6). Then there exists an $\alpha > 0$, called the *tail index* of \mathbf{X} , such that the limit measure $\nu_{\mathbf{X}}$ satisfies the homogeneity property of order α , i.e., $\nu_{\mathbf{X}}(tC) = t^{-\alpha} \nu_{\mathbf{X}}(C)$ for any constant $t > 0$ and any ($\nu_{\mathbf{X}}$ -measurable) Borel set $C \subset \mathbb{E}_0$. The sequence b_n can be shown to satisfy $b_n \sim L(n)n^{1/\alpha}$, where L denotes a slowly varying function.

The homogeneity property suggests that it is possible to express \mathbf{X} and correspondingly the limit relation in (1) in polar coordinates. Let $\|\cdot\|$ denote any norm on \mathbb{R}^d and consider the transformation $T: \mathbb{E}_0 \mapsto (0, \infty) \times \mathbb{S}_{d-1}$, where $\mathbb{S}_{d-1} = \{\mathbf{w} \in \mathbb{E}_0 : \|\mathbf{w}\| = 1\}$, and

$$T(\mathbf{X}) = \left(\|\mathbf{X}\|, \frac{\mathbf{X}}{\|\mathbf{X}\|} \right) =: (R, \mathbf{W}).$$

Then (1) is equivalent to the existence of a finite measure $H_{\mathbf{X}}$ (called the *angular measure*) on \mathbb{S}_{d-1} and a sequence $b_n \rightarrow \infty$ such that

$$(2) \quad n \mathbb{P} [(b_n^{-1} R, \mathbf{W}) \in \cdot] \xrightarrow{v} \mu_{\alpha} \times H_{\mathbf{X}}(\cdot), \quad \text{as } n \rightarrow \infty,$$

in the space of non-negative Radon measures on $(0, \infty) \times \mathbb{S}_{d-1}$, where μ_{α} is a measure on $[0, \infty)$ given by $\mu_{\alpha}((x, \infty]) = x^{-\alpha}$ for $x > 0$ (Resnick, 2007, Theorem 6.1). Let $B \subset \mathbb{S}_{d-1}$ be $H_{\mathbf{X}}$ -measurable and consider the set

$$C_{s,B} := \{\mathbf{x} \in \mathbb{E}_0 : \|\mathbf{x}\| > s, \mathbf{x}/\|\mathbf{x}\| \in B\}.$$

Equation (2) implies $\nu_{\mathbf{X}}(C_{s,B}) = s^{-\alpha} H_{\mathbf{X}}(B)$ and $\nu_{\mathbf{X}}(dr \times d\mathbf{w}) = \alpha r^{-\alpha-1} dr dH_{\mathbf{X}}(\mathbf{w})$. The angular measure $H_{\mathbf{X}}$ is related to the probability measure $S_{\mathbf{X}}$ in Resnick (2007, Chapter 6) through $H_{\mathbf{X}} = mS_{\mathbf{X}}$ for $m := \nu(C_{1,\mathbb{S}_{d-1}}) = H_{\mathbf{X}}(\mathbb{S}_{d-1}) > 0$. The sequence b_n in (2) is determined by

$$n \mathbb{P}[R > b_n x] \rightarrow m x^{-\alpha}, \quad \text{as } n \rightarrow \infty,$$

and the marginals of \mathbf{X} satisfy

$$(3) \quad \lim_{n \rightarrow \infty} n \mathbb{P}[X_j > b_n x] = x^{-\alpha} \int_{\mathbb{S}_{d-1}} w_j^\alpha dH_{\mathbf{X}}(\mathbf{w}).$$

To summarize the dependence of a multivariate regularly-varying vector \mathbf{X} , we define the *tail pairwise dependence matrix (TPDM)* $\Sigma_{\mathbf{X}}$ as

$$(4) \quad \Sigma_{\mathbf{X}} = (\sigma_{\mathbf{X}_{jk}})_{j,k=1,\dots,d}, \quad \text{with } \sigma_{\mathbf{X}_{jk}} = \int_{\mathbb{S}_{d-1}} w_j^{\alpha/2} w_k^{\alpha/2} dH_{\mathbf{X}}(\mathbf{w}).$$

Note that this constitutes a generalization of the matrix introduced in [Larsson and Resnick \(2012\)](#) whose integrand does not depend on α ; see also [Samorodnitsky and Taqqu \(1994\)](#). We will write $\mathbf{X} \sim \Sigma_{\mathbf{X}}$ if $\Sigma_{\mathbf{X}}$ is the TPDM of \mathbf{X} . When no confusion can arise, we will write the elements of $\Sigma_{\mathbf{X}}$ as σ_{jk} . Two variables X_j, X_k are *tail dependent* if and only if $\sigma_{jk} > 0$. From (3) we observe that

$$\lim_{n \rightarrow \infty} n \mathbb{P}[X_j > b_n x] = x^{-\alpha} \sigma_{jj}.$$

Hence, the (limiting) scale of X_j is $(\sigma_{jj})^{1/\alpha}$, and we say that the margins of \mathbf{X} are *standardized* with index α whenever $\sigma_{jj} = 1$ for all $j = 1, \dots, d$.

Finally, let $\|\cdot\|_\alpha$ denote the L_α norm, i.e., for $\mathbf{x} \in [0, \infty)^d$, $\|\mathbf{x}\|_\alpha = \left(\sum_{j=1}^d |x_j|^\alpha\right)^{1/\alpha}$ for $\alpha \geq 1$. In the following, we will always use the L_α norm in the definition of the angular measure $H_{\mathbf{X}}$. The total mass of the angular measure then equals

$$m = H_{\mathbf{X}}(\mathbb{S}_{d-1}) = \int_{\mathbb{S}_{d-1}} \|\mathbf{w}\|_\alpha^\alpha dH_{\mathbf{X}}(\mathbf{w}) = \sum_{j=1}^d \sigma_{jj}.$$

PROPOSITION 2.1 (Generalization of [Cooley and Thibaud \(2019\)](#)). *The tail pairwise dependence matrix $\Sigma_{\mathbf{X}}$, as defined in (4), is positive semi-definite.*

2.2. Max-linear model. We are interested in calculating the probability that \mathbf{X} falls into some extreme failure region $C \subset \mathbb{E}_0$. In practice, to estimate such probabilities $\mathbb{P}[\mathbf{X} \in C]$, we need to assume a parametric model for the exponent measure ν , or, equivalently, for the angular measure H . A simple yet effective parametric model for the goal of estimating failure probabilities is the *max-linear model*. Let A denote a $d \times q$ matrix with non-negative entries, with columns $\mathbf{a}_1, \dots, \mathbf{a}_q$, and suppose that $\max(\mathbf{a}_l) = \max(a_{1l}, \dots, a_{dl}) > 0$ for all $l \in \{1, \dots, q\}$. Let Z_1, \dots, Z_q be independent random variables whose distribution is Fréchet with scale 1 and shape α , $\mathbb{P}[Z_l \leq z] = \exp\{-z^{-\alpha}\}$, and define

$$A \times_{\max} \mathbf{Z} := \left(\max_{l=1,\dots,q} a_{1l} Z_l, \dots, \max_{l=1,\dots,q} a_{dl} Z_l \right)^T,$$

for $\mathbf{Z} = (Z_1, \dots, Z_q)$. Denoting $\mathbf{Y} = A \times_{\max} \mathbf{Z}$ and choosing $b_n = n^{1/\alpha}$, the angular measure of \mathbf{Y} is

$$(5) \quad H_{\mathbf{Y}}(\cdot) = \sum_{l=1}^q \|\mathbf{a}_l\|_\alpha^\alpha \delta_{\mathbf{a}_l / \|\mathbf{a}_l\|_\alpha}(\cdot).$$

Note that the order of the columns of A does not matter. The marginal distribution of Y_j is Fréchet with scale $\left(\sum_{l=1}^q a_{jl}^\alpha\right)^{1/\alpha}$ and shape α for $j = 1, \dots, d$. The TPDM of \mathbf{Y} has elements

$$\sigma_{\mathbf{Y}_{jk}} = \sum_{l=1}^q \|\mathbf{a}_l\|_\alpha^\alpha \left(\frac{a_{jl}}{\|\mathbf{a}_l\|_\alpha} \right)^{\alpha/2} \left(\frac{a_{kl}}{\|\mathbf{a}_l\|_\alpha} \right)^{\alpha/2} = \sum_{l=1}^q a_{jl}^{\alpha/2} a_{kl}^{\alpha/2},$$

and hence

$$\Sigma_{\mathbf{Y}} = A_* A_*^T, \quad \text{where } A_* := \left(a_{jk}^{\alpha/2} \right)_{j,k=1,\dots,d}$$

Cooley and Thibaud (2019) show that the class of max-linear angular measures, as defined in (5) is dense in the class of possible angular measures (for any norm), i.e., any multivariate regularly varying vector \mathbf{X} can be approximated by a max-linear model with a $(d \times q)$ parameter matrix as $q \rightarrow \infty$. Moreover, if attention is restricted to the TPDM, a max-linear model with *finite* q is sufficient to exactly match $\Sigma_{\mathbf{X}}$; this result has been proven in Cooley and Thibaud (2019) for $\alpha = 2$, but can be easily generalized to any $\alpha > 0$.

PROPOSITION 2.2 (Cooley and Thibaud (2019), Propositions 4 & 5).

1. Let Z_1, \dots, Z_q be Fréchet $(1, \alpha)$ random variables. Given any angular measure H , there exists a sequence of non-negative $(d \times q)$ matrices $\{A_q\}$, for $q = 1, 2, \dots$ such that $H_{A_q \times_{\max} \mathbf{Z}} \rightarrow H$ weakly as $q \rightarrow \infty$.
2. If $\mathbf{X} \in \mathbb{R}^d$ has TPDM $\Sigma_{\mathbf{X}}$, there exists a non-negative $(d \times \tilde{q})$ matrix A_* with $\tilde{q} < \infty$, such that $\Sigma_{\mathbf{X}} = A_* A_*^T = \Sigma_{A_* \times_{\max} \mathbf{Z}}$.

Whenever a matrix Σ can be decomposed as $\Sigma = AA^T$, and the matrix A has non-negative entries, we say that Σ is *completely positive*. The second part of Proposition 2.2 not only shows that the TPDM is completely positive, but also that for any vector \mathbf{X} , there exists a max-linear vector \mathbf{Y} whose TPDM is equal to that of \mathbf{X} . This result is key for the estimation of failure probabilities.

2.3. *The probability of a failure region under the max-linear model.* We intend to estimate the failure probability $\mathbb{P}[\mathbf{Y} \in C]$ for a max-linear vector \mathbf{Y} . Indeed, whenever the set $C \subset \mathbb{E}_0$ is “extreme enough”, we have

$$(6) \quad \mathbb{P}[\mathbf{Y} \in C] = \frac{1}{n} \left\{ n \mathbb{P} \left[n^{-1/\alpha} \mathbf{Y} \in n^{-1/\alpha} C \right] \right\} \approx \frac{1}{n} \nu_{\mathbf{Y}} \left(n^{-1/\alpha} C \right).$$

The choice of the region C in (6) depends on the application of interest. Nevertheless, for some practically relevant failure regions, the probability can be calculated directly from the parameters of the max-linear model. For environmental data, e.g., if \mathbf{Y} represents a vector of maximum daily wind speeds, rainfall amounts, or temperatures in d locations, the region

$$C_{(\max)}(\mathbf{x}) = \{ \mathbf{y} \in \mathbb{E}_0 : y_1 > x_1 \text{ or } \dots \text{ or } y_d > x_d \},$$

is a common choice if an extreme event at at least one location can lead to a climatological catastrophe. The exponent measure for this region equals

$$\nu(C_{(\max)}(\mathbf{x})) = \sum_{l=1}^q \max_{j=1,\dots,d} \left(\frac{a_{jl}}{x_j} \right)^\alpha.$$

On the other hand, if \mathbf{Y} represents for example the negative log-returns of d stocks in a portfolio, one might be interested in estimating the probability of all stocks crashing together,

$$C_{(\min)}(\mathbf{x}) = \{ \mathbf{y} \in \mathbb{E}_0 : y_1 > x_1 \text{ and } \dots \text{ and } y_d > x_d \}.$$

Similarly to $C_{(\max)}$, we can calculate

$$\nu(C_{(\min)}(\mathbf{x})) = \sum_{l=1}^q \min_{j=1,\dots,d} \left(\frac{a_{jl}}{x_j} \right)^\alpha.$$

Many simple regions (including the ones above when $x_1 = \dots = x_d$) can be written as follows. Let $C_f(x) = \{\mathbf{y} \in \mathbb{E}_0 : f(\mathbf{y}) > x\}$ denote a failure region where $f : \mathbb{R}^d \rightarrow \mathbb{R}$ is some function. For fixed w , let $r_* = r_*(w)$ be such that $f(r_*w) = x$. Then

$$\nu(C_f(x)) = \sum_{l=1}^q \|\mathbf{a}_l\|_\alpha^\alpha \{r_*(\mathbf{a}_l/\|\mathbf{a}_l\|_\alpha)\}^{-\alpha}.$$

Hence, we can obtain an explicit expression for the exponent measure of any failure region that can be written in the form of C_f . For example, if $f(\mathbf{y}) = \mathbf{v}^T \mathbf{y}$ for $\mathbf{v} \in \mathbb{E}_0$ such that $v_1 + \dots + v_d = 1$, we get

$$C_{(\text{sum})}(\mathbf{v}, x) = \{\mathbf{y} \in \mathbb{E}_0 : v_1 y_1 + \dots + v_d y_d > x\}.$$

Such a region is both of interest for climate events (e.g. in attribution studies such as [Kiriliouk and Naveau \(2020\)](#), among others) and in the financial context (e.g. to calculate the Value-at-Risk for a portfolio), and we calculate

$$\nu(C_{(\text{sum})}(\mathbf{v}, x)) = x^{-\alpha} \sum_{l=1}^q (\mathbf{v}^T \mathbf{a}_l)^\alpha.$$

Moreover, we find

$$\nu(C_{(\text{sum})}(\mathbf{v}, x)) = \begin{cases} x^{-1} \sum_{j=1}^d v_j \sigma_{jj} & \text{if } \alpha = 1, \\ x^{-2} (\mathbf{v}^T \Sigma_{\mathbf{X}} \mathbf{v}) & \text{if } \alpha = 2. \end{cases}$$

In these two special cases, $\nu(C_{(\text{sum})}(\mathbf{v}, x))$ can be calculated based on the TPDM only. In other words, the random variable $\mathbf{v}^T \mathbf{Y}$ approximately follows a Pareto distribution whose scale is a function of the TPDM. By contrast, when $\alpha \notin \{1, 2\}$, the parameter matrix A needs to be recovered first.

3. Decomposing the pairwise tail dependence matrix. Proposition 2.2 shows that, for any random vector \mathbf{X} , a max-linear vector \mathbf{Y} exists such that $\Sigma_{\mathbf{X}} = \Sigma_{\mathbf{Y}}$. Obtaining such a model requires a *completely positive decomposition* of $\Sigma_{\mathbf{X}}$, i.e., finding a $(d \times q)$ matrix A_* with non-negative entries such that $\Sigma_{\mathbf{X}} = A_* A_*^T$ (see also Section 2.2). [Barioli and Berman \(2003\)](#) show that the number of columns of such a matrix A_* is at most $d(d+1)/2 - 4$ for $d \geq 5$. Current algorithms performing completely positive decompositions are computationally heavy ([Groetzner and Dür, 2020](#); [Boğ and Nguyen, 2021](#)), and hence they cannot be applied repeatedly to obtain multiple factorizations when the dimension d is high. Notice that the factorization of a completely positive matrix is not unique. Obtaining multiple different decompositions could be useful to quantify the model uncertainty regarding estimations of the probability of falling into a failure region.

In this section, we propose a simple algorithm to construct a $(d \times d)$ matrix A_* , which leads to an *approximate* completely positive decomposition in the following sense. Firstly, we define the notation “ \preceq ”: for two TPDMs, we write $\Sigma_{\mathbf{X}} \preceq \Sigma_{\mathbf{Y}}$ if

$$\sigma_{\mathbf{X}_{jk}} = \sigma_{\mathbf{Y}_{jk}} \quad \text{for all } j, k \in \{1, \dots, d\}, j \neq k, \quad \text{and } \sigma_{\mathbf{X}_{jj}} \leq \sigma_{\mathbf{Y}_{jj}} \quad \text{for all } j \in \{1, \dots, d\}.$$

Then, for any random vector \mathbf{X} with TPDM $\Sigma_{\mathbf{X}}$, we aim at constructing a max-linear vector \mathbf{Y} with a $(d \times d)$ coefficient matrix A_* , such that $\Sigma_{\mathbf{X}} \preceq \Sigma_{\mathbf{Y}}$. The max-linear model can be viewed as an approximate model for the original random vector \mathbf{X} , “matching” the pairwise dependence structure of \mathbf{X} .

The details of the proposed algorithm are as follows. Define, for any TPDM $\Sigma_{\mathbf{X}} = (\sigma_{jk})_{j,k=1,\dots,d}$ and any $i \in \{1, \dots, d\}$,

$$D_i(\Sigma_{\mathbf{X}}) := \max \left\{ j, k \in \{1, \dots, d\} \setminus \{i\} : \frac{\sigma_{ji}\sigma_{ki}}{\sigma_{jk}\sigma_{ii}} \right\}.$$

We write $D_i = D_i(\Sigma_{\mathbf{X}})$ when no confusion can arise. Let $\tau_i = (\tau_{1,i}, \dots, \tau_{d,i})^T$ with

$$(7) \quad \tau_{j,i} = \begin{cases} \sigma_{ji} (\sigma_{ii} \max(D_i, 1))^{-1/2} & \text{if } j \neq i, \\ (\sigma_{ii} \max(D_i, 1))^{1/2} & \text{if } j = i. \end{cases}$$

Let $\tau_{-i} := (\tau_{1,i}, \dots, \tau_{i-1,i}, \tau_{i+1,i}, \dots, \tau_{d,i})^T \in \mathbb{R}^{d-1}$ and define

$$(8) \quad \Sigma_{\mathbf{X}}^{(i)} := \Sigma_{\mathbf{X}}^{(-i,-i)} - \tau_{-i} \tau_{-i}^T \in \mathbb{R}^{(d-1) \times (d-1)},$$

where $\Sigma_{\mathbf{X}}^{(-i,-i)} \in \mathbb{R}^{(d-1) \times (d-1)}$ is the matrix obtained by removing the i -th row and column from $\Sigma_{\mathbf{X}}$. The following lemma shows that $\Sigma_{\mathbf{X}}^{(i)}$ is still a valid TPDM.

LEMMA 3.1. *For all $i \in \{1, \dots, d\}$ with $D_i \neq 1$, the matrix $\Sigma_{\mathbf{X}}^{(i)}$ in (8) is a TPDM since*

1. $\Sigma_{\mathbf{X}}^{(i)} > 0$ componentwise;
2. $\Sigma_{\mathbf{X}}^{(i)}$ is positive semi-definite.

The next proposition shows that if we can construct a $(d-1)$ -dimensional random vector with TPDM $\Sigma_{\mathbf{X}}^{(i)}$, we can then use this vector to construct \mathbf{Y} such that $\Sigma_{\mathbf{X}} \preceq \Sigma_{\mathbf{Y}}$. In addition, the proposition illustrates the circumstances under which $\Sigma_{\mathbf{X}} = \Sigma_{\mathbf{Y}}$ is achieved. The proofs of Lemma 3.1 and of Proposition 3.2 are postponed to the appendix.

PROPOSITION 3.2. *Let $\Sigma_{\mathbf{X}} = (\sigma_{jk})_{j,k=1,\dots,d} \in \mathbb{R}^{d \times d}$ be a TPDM. Let $i \in \{1, \dots, d\}$ and let Z_i be a Fréchet random variable with scale 1 and shape α . Suppose there exists a random vector $\tilde{\mathbf{Y}}_{-i} = (\tilde{Y}_1, \dots, \tilde{Y}_{i-1}, \tilde{Y}_{i+1}, \dots, \tilde{Y}_d)^T$ with TPDM $\Sigma_{\mathbf{X}}^{(i)}$. By defining*

$$Y_j := \begin{cases} \max \left(\tau_{j,i}^{2/\alpha} Z_i, \tilde{Y}_j \right) & \text{if } j \in \{1, \dots, d\} \setminus \{i\}, \\ \tau_{i,i}^{2/\alpha} Z_i & \text{if } j = i, \end{cases}$$

we have that $\Sigma_{\mathbf{X}} \preceq \Sigma_{\mathbf{Y}}$. In particular, if $D_i(\Sigma_{\mathbf{X}}) < 1$, then $\Sigma_{\mathbf{Y}} = \Sigma_{\mathbf{X}}$.

Hence, we can repeatedly apply the procedure in expression (8) to $\Sigma_{\mathbf{X}}^{(i)}$ to further decrease the dimension. This leads to an iterative algorithm, throughout which we obtain the matrix A_* . First, let $i_1 \mapsto i_2 \mapsto \dots \mapsto i_d$ denote a *path*, where (i_1, \dots, i_d) is a permutation of $(1, \dots, d)$. The order determines which column of $\Sigma_{\mathbf{X}}$ will be treated first using Proposition 3.2. For a given path, the iterative algorithm is as follows.

- In the first step, we obtain the vector τ_{i_1} from (7) by taking $i = i_1$. We fill in the first column of the matrix A_* with the obtained vector τ_{i_1} (as the order of the columns of A_* does not matter, we do not necessarily need to fill the i_1 -th column). The targeted TPDM is then reduced to a $(d-1) \times (d-1)$ matrix $\Sigma_{\mathbf{X}}^{(-i_1)}$ as defined in (8).
- In the second step, we apply expressions (7) and (8) to $\Sigma_{\mathbf{X}}^{(-i_1)}$, with the focal dimension now indexed by i_2 . This step results in a $(d-1)$ -dimensional vector. For the second column of the matrix A_* , we set the i_1 -th row to zero and fill in the rest with the obtained $(d-1)$ -dimensional vector. After the second step, the targeted TPDM is reduced to a $(d-2) \times (d-2)$ matrix.

- The previous step is iterated as follows. In each step j , we aim at filling in the j -th column of the matrix A_* . First, we set the elements in the i_1, i_2, \dots, i_{j-1} -th row to zero. Then, we fill in the other $(d - j + 1)$ elements by the obtained $(d - j + 1)$ -dimensional vector of this iteration. After each step, the dimension of the targeted TPDM is reduced by one.
- At step d , the targeted TPDM is reduced to 1×1 , i.e. a single positive number. We simply fill in the square root of that value to the d -th column and i_d -th row of A_* , while setting all other elements in the d -th column to zero.

Proposition 3.2 guarantees that the matrix A_* obtained with this algorithm has only non-negative elements and satisfies $\Sigma_{\mathbf{X}} \preceq A_* A_*^T$. In addition, define $A = A_*^{2/\alpha}$ (i.e. each element of the matrix A_* is raised to the power $2/\alpha$) and let $\mathbf{Z} = (Z_1, \dots, Z_d)^T$ where Z_1, \dots, Z_d are i.i.d. standard Fréchet distributed random variables with scale 1 and shape α . The max-linear vector $\mathbf{Y} = A \times_{\max} \mathbf{Z}$ has a TPDM that satisfies $\Sigma_{\mathbf{X}} \preceq \Sigma_{\mathbf{Y}}$. In other words, we can construct a max-linear vector \mathbf{Y} based on only d independent factors to approximate the TPDM of \mathbf{X} .

Below is an example for this procedure when $d = 3$ and the chosen path is $1 \mapsto 2 \mapsto 3$.

EXAMPLE 3.3 ($d = 3, \alpha = 2$, path $1 \mapsto 2 \mapsto 3$). Let $\Sigma_{\mathbf{X}} = (\sigma_{jk})_{j,k=1,2,3}$ be a known (or estimated) TPDM. We want to find a coefficient matrix A (since $\alpha = 2$, we have $A = A_*$) such that the corresponding max-linear model $\mathbf{Y} = A \times_{\max} (Z_1, Z_2, Z_3)^T$ has TPDM $\Sigma_{\mathbf{Y}}$ satisfying $\Sigma_{\mathbf{X}} \preceq \Sigma_{\mathbf{Y}}$. Starting with $i = 1$, we obtain from (7) that

$$\begin{pmatrix} \tau_{1,1} \\ \tau_{2,1} \\ \tau_{3,1} \end{pmatrix} = \frac{1}{\sqrt{\sigma_{11} \max(D_1, 1)}} \begin{pmatrix} \sigma_{11} \max(D_1, 1) \\ \sigma_{12} \\ \sigma_{13} \end{pmatrix}$$

and

$$\Sigma_{\mathbf{X}}^{(-1)} := \begin{pmatrix} s_{22} & s_{23} \\ s_{23} & s_{33} \end{pmatrix} := \begin{pmatrix} \sigma_{22} - \frac{\sigma_{12}^2}{\sigma_{11} \max(D_1, 1)} & \sigma_{23} - \frac{\sigma_{12}\sigma_{13}}{\sigma_{11} \max(D_1, 1)} \\ \sigma_{23} - \frac{\sigma_{12}\sigma_{13}}{\sigma_{11} \max(D_1, 1)} & \sigma_{33} - \frac{\sigma_{13}^2}{\sigma_{11} \max(D_1, 1)} \end{pmatrix}.$$

Hence, the first column of A is given by $(\tau_{1,1}, \tau_{2,1}, \tau_{3,1})^T$.

To find the second column of A , we iterate the same algorithm to the newly obtained TPDM $\Sigma_{\mathbf{X}}^{(-1)}$ to get that

$$\begin{pmatrix} \tau_{2,2} \\ \tau_{3,2} \end{pmatrix} = \frac{1}{\sqrt{s_{22}}} \begin{pmatrix} s_{22} \\ s_{23} \end{pmatrix}.$$

Note that since $\Sigma_{\mathbf{X}}^{(-1)}$ is positive semidefinite, in this case we have $D_2(\Sigma_{\mathbf{X}}^{(-1)}) = \frac{s_{23}^2}{s_{33}s_{22}} \leq 1$. After this iteration, the targeted TPDM is reduced to a single value $s_{33} - s_{23}^2/s_{22} \geq 0$. Hence, we can define $\tau_{3,3} := \sqrt{s_{33} - s_{23}^2/s_{22}}$.

Eventually, we can construct the max-linear model as $\mathbf{Y} = A \times_{\max} (Z_1, Z_2, Z_3)$ where

$$A = \begin{pmatrix} \tau_{1,1} & 0 & 0 \\ \tau_{2,1} & \tau_{2,2} & 0 \\ \tau_{3,1} & \tau_{3,2} & \tau_{3,3} \end{pmatrix}, \quad \text{and} \quad \Sigma_{\mathbf{Y}} = AA^T = \begin{pmatrix} \sigma_{11} \max(D_1, 1) & \sigma_{12} & \sigma_{13} \\ \sigma_{12} & \sigma_{22} & \sigma_{23} \\ \sigma_{13} & \sigma_{23} & \sigma_{33} \end{pmatrix}.$$

We have that $\Sigma_{\mathbf{Y}} = \Sigma_{\mathbf{X}}$ if $D_1 < 1$ and $\Sigma_{\mathbf{X}} \preceq \Sigma_{\mathbf{Y}}$ otherwise.

If the matrix $\Sigma_{\mathbf{X}}$ has a zero eigenvalue, it means that the components of \mathbf{X} are linearly related when the radius R is high. In practice, an eigenvalue of $\Sigma_{\mathbf{X}}$ can indeed be close to zero when the variables are strongly dependent given a high radius. This is comparable with the concept of multicollinearity in multivariate statistics. In that case, at least one column of A_* will be zero: the column corresponding to the first variable encountered that is close to a

linear combination of previous variables, given that the radius is high. We can remove that column in A_* and correspondingly A . Eventually, the number of non-zero columns of A_* corresponds to the rank of $\Sigma_{\mathbf{X}}$.

In Example 3.3, we applied the iterative algorithm implied by Proposition 3.2 with the path $1 \mapsto 2 \mapsto 3$. The resulting matrix A_* (and eventually A) is then lower triangular. By considering others paths we will obtain different matrices A_* . Hence, in general, for different choices of paths, a completely positive decomposition (approximate or not) is not unique. It is also possible that one path leads to an exact decomposition while another path leads to an approximation in the sense of \preceq . Proposition 3.4 shows that if the vector \mathbf{X} indeed follows a max-linear model constructed from a lower-triangular parameter matrix A , by choosing the path *appropriately*, it is possible to recover the exact max-linear model. Given that the order of columns of A does not matter, the proposition can of course be generalized to parameter matrices A in which each column j has at least one more zero than column $(j - 1)$, for $j = 2, \dots, d$.

PROPOSITION 3.4. *Suppose that $\mathbf{X} = A \times_{\max} \mathbf{Z}$ follows a max-linear model with lower-triangular parameter matrix $A \in \mathbb{R}^{d \times d}$ and $\mathbf{Z} = (Z_1, \dots, Z_d)$, where Z_1, \dots, Z_d are iid Fréchet with scale 1 and shape α . If we choose the canonical path, i.e., $1 \mapsto \dots \mapsto d$ in the decomposition of $\Sigma_{\mathbf{X}}$ to obtain the matrix A_* , then $A_* A_*^T = \Sigma_{\mathbf{X}}$.*

For a high-dimensional TPDM $\Sigma_{\mathbf{X}}$, it is not feasible to exhaust all $d!$ possible paths in search for an exact decomposition. In practice, we need an efficient searching algorithm to find a path that leads to a max-linear model \mathbf{Y} such that $\Sigma_{\mathbf{Y}} = \Sigma_{\mathbf{X}}$, if possible. We consider three potential algorithms to achieve the goal.

1. A simple approach: In step j we pick the next dimension i_j corresponding to the lowest value of D_i among all remaining dimensions.
2. An exhaustive approach: In step j , we denote T_j as the *set* of remaining dimensions corresponding to a value of D_i below 1, i.e. $T_j := \{i : D_i < 1, i \neq i_1, i_2, \dots, i_{j-1}\}$. For each $i \in T_j$, we proceed with the iterative process for $\Sigma_{\mathbf{X}}^{(-i)}$. This will result in a tree of possibilities after each step. For some “branches” of the tree, the algorithm may end at a “leaf” where no D_i lies below 1, i.e. $T_j = \emptyset$. If some “branch” can iterate d steps, it leads to a path that corresponds to an exact decomposition. We retain all paths (and hence all possible matrices A_*) that lead to an exact decomposition.
3. A pragmatic approach: In step j , we denote T_j as the *set* of remaining dimensions corresponding to a value of D_i below 1, i.e. $T_j := \{i : D_i < 1, i \neq i_1, i_2, \dots, i_{j-1}\}$. We randomly choose a dimension from this set as i_j and proceed with the iteration. If the procedure stops after less than d iterations and ends with a scenario where no D_i lies below 1, we restart the entire procedure from the first iteration. We keep “restarting” the algorithm until finding an exact decomposition.

Note that the simple approach may not lead to an exact decomposition because there is no guarantee that the minimum of the D_i 's is below 1 in all steps. The exhaustive approach will find all exact decompositions if there exists at least one. However, it is limited to moderate dimensions d because of its computational intensity. The pragmatic approach does not guarantee finding an exact decomposition either. Nevertheless, for most examples in Section 5, an exact decomposition is quickly found after a few “restarts”, and hence it is the approach that we will most use in practice.

4. Estimation.

4.1. *Estimation of the TPDM.* Let $\mathbf{X}_i = (X_{i1}, \dots, X_{id})$ for $i = 1, \dots, n$ be iid copies of \mathbf{X} . First, we estimate the tail indices α_j , or, equivalently, the extreme value indices $\gamma_j = 1/\alpha_j$, for each $j = 1, \dots, d$ using the sample $\{X_{1j}, \dots, X_{nj}\}$. Note that the assumption of regular variation (1) implies that all margins have equal tail indices, $\alpha_1 = \dots = \alpha_d := \alpha$, which is a common assumption, since different tail indices will lead to the largest one dominating the others and masking tail dependence.

Let $X_{(1),j} \leq \dots \leq X_{(n),j}$ denote the order statistics of X_{1j}, \dots, X_{nj} and let $k = k_n$ be an intermediate sequence such that $k \rightarrow \infty$ and $k/n \rightarrow 0$ as $n \rightarrow \infty$. The *Hill estimator*,

$$\widehat{\gamma}_j = \frac{1}{k} \sum_{i=1}^k \log \left(\frac{X_{(n-i+1),j}}{X_{(n-k),j}} \right)$$

is the best-known estimator of the extreme-value index (Hill, 1975), and will be used to obtain the estimated tail indices $\widehat{\alpha}_j = 1/\widehat{\gamma}_j$. If the confidence intervals of $\widehat{\alpha}_1, \dots, \widehat{\alpha}_d$ are overlapping, a single tail index estimate $\widehat{\alpha}$ might be justified. In that case, the entire sample $X_{11}, \dots, X_{n1}, X_{12}, \dots, X_{n2}, \dots, X_{1d}, \dots, X_{nd}$ of length nd can be used to obtain the estimate $\widehat{\alpha}$ (Einmahl et al., 2022).

Next, for $i = 1, \dots, n$, set $R_i = \|\mathbf{X}_i\|_{\widehat{\alpha}}$ and $\mathbf{W}_i = \mathbf{X}_i/R_i$. Let $m = H_{\mathbf{X}}(\mathbb{S}_{d-1})$ denote the total mass of the angular measure. If the data are standardized to ensure equal scales for all j (see subsection 4.2), then $m = d$. Otherwise, we observe that

$$m = \nu_{\mathbf{X}}(C_{1,\mathbb{S}_{d-1}}) = \lim_{n \rightarrow \infty} n \mathbb{P}[b_n^{-1} \mathbf{X}_i \in C_{1,\mathbb{S}_{d-1}}] = \lim_{n \rightarrow \infty} n \mathbb{P}[R_i > b_n]$$

Following Cooley and Thibaud (2019), we estimate b_n by a high quantile of the empirical distribution of R_1, \dots, R_n , denoted as r_0 . By setting $n \approx r_0^{\widehat{\alpha}}$, m can be estimated by $\widehat{m} = r_0^{\widehat{\alpha}}(n_{\text{exc}}/n)$ for $n_{\text{exc}} = \sum_{i=1}^n \mathbb{1}\{R_i > r_0\}$. A value for r_0 could be chosen by plotting different quantiles against the estimates of m and searching for a region where estimates are stable. Finally, since $\sigma_{jk} = m \int_{\mathbb{S}_{d-1}} w_j^{\alpha/2} w_k^{\alpha/2} d\widetilde{H}_{\mathbf{X}}(\mathbf{w})$ where $\widetilde{H}_{\mathbf{X}}(\cdot) := m^{-1}H_{\mathbf{X}}(\cdot)$ is a probability measure, the elements of the TPDM can be estimated by

$$\widehat{\sigma}_{jk} = \frac{\widehat{m}}{n_{\text{exc}}} \sum_{i=1}^n W_{ij}^{\widehat{\alpha}/2} W_{ik}^{\widehat{\alpha}/2} \mathbb{1}\{R_i > r_0\} = \frac{r_0^{\widehat{\alpha}}}{n} \sum_{i:R_i > r_0} (W_{ij} W_{ik})^{\widehat{\alpha}/2},$$

giving $\widehat{\Sigma}_{\mathbf{X}} = (\widehat{\sigma}_{jk})_{j,k=1,\dots,d}$. Larsson and Resnick (2012) show the asymptotic normality of $\widehat{\sigma}_{jk}$ when $\alpha = 2$ is known.

4.2. *Estimation of failure probabilities and standardization.* Once the TPDM is estimated, we calculate the $d \times d$ matrix \widehat{A}_* obtained by applying the decomposition algorithm outlined in Section 3 to $\widehat{\Sigma}_{\mathbf{X}}$, and the empirical $(d \times n_{\text{exc}})$ estimate

$$\widetilde{A}_* = \left(\frac{\widehat{m}}{n_{\text{exc}}} \right)^{1/2} \widehat{W}^{\widehat{\alpha}/2},$$

where $\widehat{W}^{\widehat{\alpha}/2}$ is the matrix whose columns are the vectors $\mathbf{W}_i^{\widehat{\alpha}/2}$ for which $R_i > r_0$. The matrix \widetilde{A}_* is “inefficient” in the sense that it has much more columns than \widehat{A}_* , especially when n_{exc} is large. However, it is easy to calculate and satisfies $\widehat{\Sigma}_{\mathbf{X}} = \widetilde{A}_* \widetilde{A}_*^T$; we will use it as a benchmark. We obtain two estimators of A as

$$\widetilde{A} = \left(\widetilde{A}_* \right)^{2/\widehat{\alpha}} \quad \text{and} \quad \widehat{A} = \left(\widehat{A}_* \right)^{2/\widehat{\alpha}}.$$

Now, \tilde{A} and \hat{A} can be used to estimate the probability of falling into one of the failure regions presented in Section 2.3. We will denote the estimators of these probabilities by \hat{p} for \tilde{A} and \tilde{p} for \hat{A} . In the applications, we will usually take the pragmatic approach described in Section 3 to generate N different matrices $\hat{A}_{*1}, \dots, \hat{A}_{*N}$ that correspond to *exact* decompositions of $\hat{\Sigma}_{\mathbf{X}}$. By an exact decomposition, we mean that $\|\hat{\Sigma}_{\mathbf{X}} - \hat{A}_{*l}\hat{A}_{*l}^T\|_F \leq 10^{-12}$ for some $l = 1, \dots, N$, where $\|\cdot\|_F$ denotes the Frobenius norm.

Finally, note that for certain failure regions we could standardize the margins of $\mathbf{X}_1, \dots, \mathbf{X}_n$ without losing tractability of the shape of the failure set. We set

$$X_{ij}^{\#} = h_j(X_{ij}) = \left(-\log \hat{F}_j^P(X_{ij})\right)^{-1/2}, \quad j = 1, \dots, d, i = 1, \dots, n,$$

where \hat{F}_j^P denotes the semi-parametric estimate of F_j ,

$$\hat{F}_j^P(y) = \begin{cases} \hat{F}_j(y) & \text{if } y \leq u_j; \\ 1 - \left(1 - \hat{F}_j(u_j)\right) \bar{H}_{\hat{\sigma}_j, \hat{\gamma}_j}(y - u_j) & \text{if } y > u_j; \end{cases}$$

where \hat{F}_j denotes the empirical distribution function of X_{1j}, \dots, X_{nj} and $\bar{H}_{\hat{\sigma}_j, \hat{\gamma}_j}$ the survival function of a generalized Pareto distribution (GPD) with estimated scale $\hat{\sigma}_j$ and shape $\hat{\gamma}_j$, obtained by fitting $(X_{ij} - u_j \mid X_{ij} > u_j)_{i=1, \dots, n}$ to the GPD for some high threshold u_j . The distribution of $X_{1j}^{\#}, \dots, X_{nj}^{\#}$ is Fréchet with scale 1 and shape $\alpha = 2$. Hence, we have $\sigma_{jj} = 1$ for $j \in \{1, \dots, d\}$ and $m = H_{\mathbf{X}}(\mathbb{S}_{d-1}) = d$ does not need to be estimated. Subsequently, we can decompose the TPDM $\hat{\Sigma}_{\mathbf{X}^{\#}}$ and construct the associated max-linear model.

5. Applications.

5.1. *Failure probabilities computed from repeated decompositions.* The TPDM forms an incomplete characterization of tail dependence; hence, we would like to assess by how much the exponent measure of a given failure region varies if it is computed from repeated decompositions. We proceed as follows, inspired by Section 2 of the supplementary material of [Cooley and Thibaud \(2019\)](#). Let

$$A_1 = \begin{pmatrix} 1.00 & 0.50 & 1.75 & 0.00 & 0.50 & 0.75 & 1.00 & 0.25 \\ 2.00 & 0.00 & 1.00 & 1.50 & 0.25 & 1.00 & 1.00 & 1.00 \\ 1.75 & 1.25 & 0.50 & 0.75 & 2.00 & 1.75 & 0.25 & 0.25 \\ 1.25 & 0.25 & 1.25 & 2.00 & 2.00 & 0.50 & 0.25 & 0.25 \\ 1.75 & 0.50 & 0.25 & 0.75 & 0.50 & 1.75 & 0.00 & 1.25 \end{pmatrix},$$

$$A_2 = \begin{pmatrix} 1.00 & 0.00 & 0.50 & 0.00 & 0.50 \\ 2.00 & 1.50 & 0.00 & 1.00 & 0.00 \\ 1.75 & 0.75 & 1.25 & 0.25 & 0.75 \\ 1.25 & 2.00 & 0.25 & 0.25 & 0.25 \\ 1.75 & 0.75 & 0.50 & 1.25 & 0.50 \end{pmatrix}, \quad \text{and } A_3 = \begin{pmatrix} 1.00 & 0.00 & 0.00 \\ 2.00 & 1.50 & 0.00 \\ 1.75 & 0.75 & 0.25 \\ 1.25 & 2.00 & 1.00 \\ 1.75 & 0.75 & 0.50 \end{pmatrix}$$

Matrix A_1 is as in [Cooley and Thibaud \(2019\)](#) (randomly generated elements). Matrices A_2 and A_3 are similar but contain less columns and more zeroes; hence, we expect to obtain more exact decompositions for A_2 and A_3 than for A_1 . Let ν_i denote the exponent measure of a max-linear random vector with coefficient matrix A_i , $i = 1, 2, 3$ and $\alpha = 4$. Let $\Sigma_i = A_i A_i^T$; we obtain the $d! = 5! = 120$ decompositions of Σ_i and consider the 120 max-linear vectors with corresponding coefficient matrices for each $i = 1, 2, 3$. From the 120 possible paths, we use only 94 paths for A_1 , 86 for A_2 , and 88 for A_3 , since the others lead to paths with $D_i = 1$; see Section 3.

We assess the limiting exponent measure of $C_f(x) = \{\mathbf{y} \in \mathbb{E}_0 : f(\mathbf{y}) > x\}$ where f is some function; see Section 2.3. We use the functions $f_1(\mathbf{y}) = \frac{1}{d} \sum_{j=1}^d y_j$, $f_2(\mathbf{y}) = \prod_{j=1}^d y_j$, $f_3(\mathbf{y}) = \min(y_1, \dots, y_d)$ and $f_4(\mathbf{y}) = \max(y_1, \dots, y_d)$. We take $\alpha = 4$ and x is always chosen such that $\nu_j(C_f) = 0.1$. Figure 1 shows boxplots for the measures ν_i , $i = 1, 2, 3$, of the sets $C_{f_1}, C_{f_2}, C_{f_3}$ and C_{f_4} , obtained through the different paths. We show both the results when taking only exact decompositions into account (12 for A_1 , 16 for A_2 , and 24 for A_3) and when taking all decompositions such that $\|\Sigma_X - AA^T\|_F \leq 5$ (58 for A_1 , 72 for A_2 , and 76 for A_3). For A_3 , 24 decompositions contain only 3 columns and are exactly equal to A_3 , while 40 other decompositions contain 4 columns. For the product-region (f_2) and the min-region (f_3), only the first column of the obtained coefficient matrices is used in the calculation of ν_i (since all subsequent columns contain at least one zero; see also Section 2.3). Overall, the TPDM seems a reasonable summary of tail dependence. We see that the tail dependence properties of the failure regions based on f_1 and f_4 are better summarized through the TPDM than those of the failure regions based on f_2 and f_3 . This can be explained by the fact that the regions C_{f_1} and C_{f_4} “cut” the axes and hence concern more scenarios than the regions C_{f_2} and C_{f_3} that only concern scenarios involving simultaneous extremes. In general, variability increases when using approximate decompositions rather than exact decompositions.

5.2. Wind gusts in the Netherlands. Extreme windstorms are one of the important natural hazards affecting Europe. Impacts are not primarily caused by wind speed itself but by the gusts, i.e., the maxima of the wind speed during a few seconds. In February 2022, storm Eunice caused massive damages in Western, Central, and Northern Europe. In the Netherlands, the maximum wind gust measured during storm Eunice was 144 km/h at station Cabauw, which set the record for harshest inland wind to have ever been measured in the Netherlands.

We consider daily maximal speeds of wind gusts, measured in km/h, observed at $d = 35$ weather stations in the Netherlands during extended winter (October–March), from October 2001 up to and including March 2022. The data set is freely available from the Royal Netherlands Meteorological Institute (KNMI), <https://climexp.knmi.nl/>. Please note that up to 50 stations are available in the Netherlands, but 15 were removed because of a large amount of missing data. The remaining 35 stations have between 0 and 15 missing data points out of $n = 3827$; these do not occur around clusters of extreme wind gusts and hence they do not impact the following analysis. During the extended winter season, the KNMI issues a code red alarm (for any Dutch province) when there is at least 90 % certitude that wind gusts will exceed 120 km/h. The 35 weather stations are initially divided into coastal stations (17) and inland stations (18) based on the same criteria used in Lenderink, Van Meijgaard and Selten (2009), because most environmental variables are known to behave differently over land or close to the sea; see Figure 3 (left) for a map of the stations used in this study.

We first estimate the marginal tail indices $\alpha_j = 1/\gamma_j$ using the standard Hill estimator with automated threshold selection (the so-called “automated eye-ball method” in Danielsson et al. (2016), where we consider $k \geq 15$). However, the Hill estimator is very erratic because of the many ties present in the data (due to rounding). To overcome this issue, we calculate the smoothed Hill estimator (Resnick and Stărică, 1997) before applying the automated eye-ball method to choose a threshold. Figure 2 (right) shows the estimates, with upper and lower bootstrap confidence limits for a 95% confidence level, obtained through a block bootstrap using the R package boot (Canty and Ripley, 2020). The first 17 bars correspond to coastal stations, the following 18 bars to inland stations. We see no apparent differences between the tail heaviness of maximum wind gusts at the coast and inland. The horizontal line shows the smoothed Hill estimate $\hat{\alpha} = 9.289$ (where k is again chosen following the automated eye-ball method), based on pooling all data from the 35 weather stations.

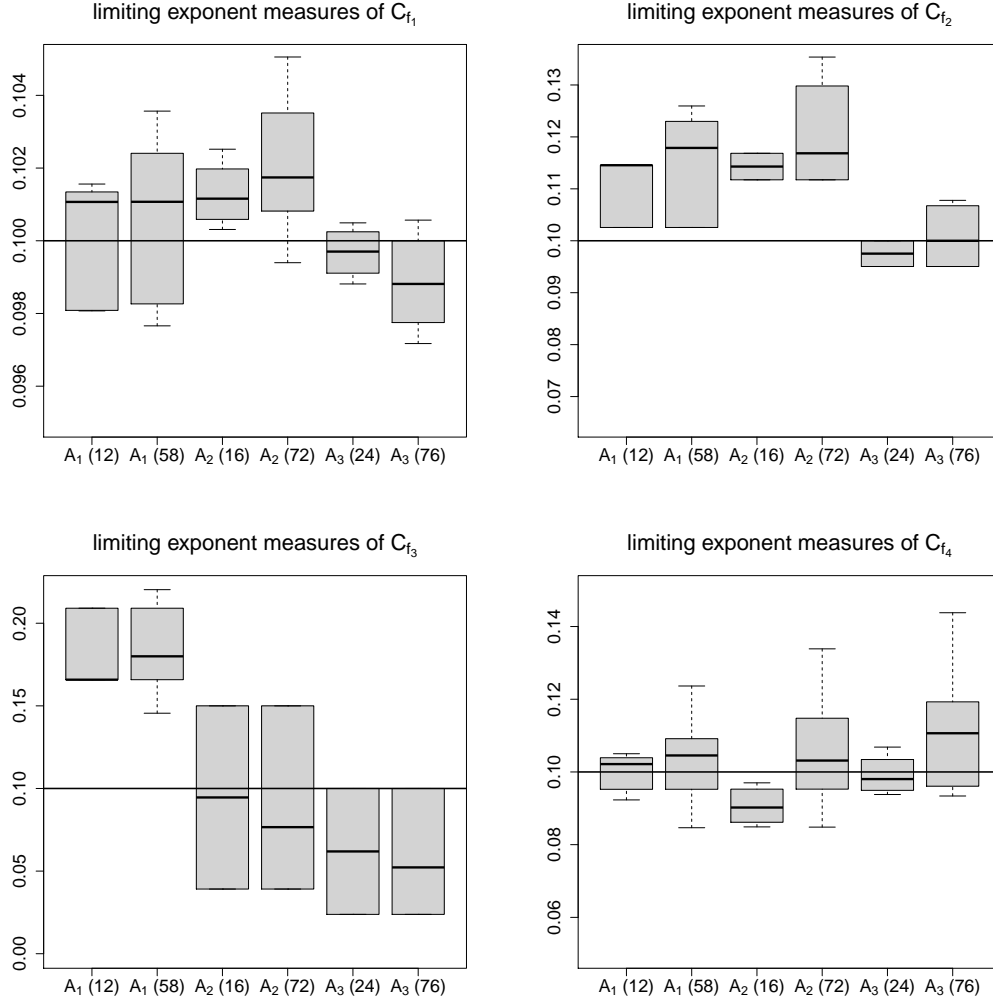


Fig 1: Boxplots of limiting exponent measures of exact and approximate decompositions of Σ_1 , Σ_2 , Σ_3 and Σ_4 for the four functions f_1 , f_2 , f_3 , and f_4 , and $\alpha = 4$. The numbers in parentheses represent the number of decompositions on which the boxplot is based.

The next step concerns the choice of r_0 . Figure 2 (right) show estimates of m , the total mass of the angular measure, as a function of r_0 . We continue with r_0 corresponding to the 95% quantile and hence $\hat{m} = 0.175$, corresponding to using the 192 largest values.

Next, we estimate pairwise tail dependence coefficients non-parametrically to examine the difference in pairwise dependence structure between the coastal and the inland stations. Figure 3 shows both the pairwise tail dependence coefficients χ_{jk} (middle) and the tail pairwise dependence matrix entries σ_{jk} (right), for $j, k = 1, \dots, d$. The plot suggests that there is no significant difference between pairs of inland or pairs of coastal stations, and that the wind gusts are asymptotically dependent, even for large distances.

Finally, we estimate A as described in Section 4.2; in total, we obtain $N = 200$ exact decompositions of $\hat{\Sigma}_{\mathbf{X}}$. Based on \tilde{A} and on $\hat{A}_1, \dots, \hat{A}_{200}$, we estimate the probability $p_{(\max)} = \mathbb{P}[\mathbf{X} \in C_{\max}(\mathbf{x})]$ for $\mathbf{x} = x\mathbf{1}_d$ and $x \in \{1, 1.2, 1.44\}$; the first two values are the thresholds for a code orange and a code red alarm respectively (issued by the KNMI during

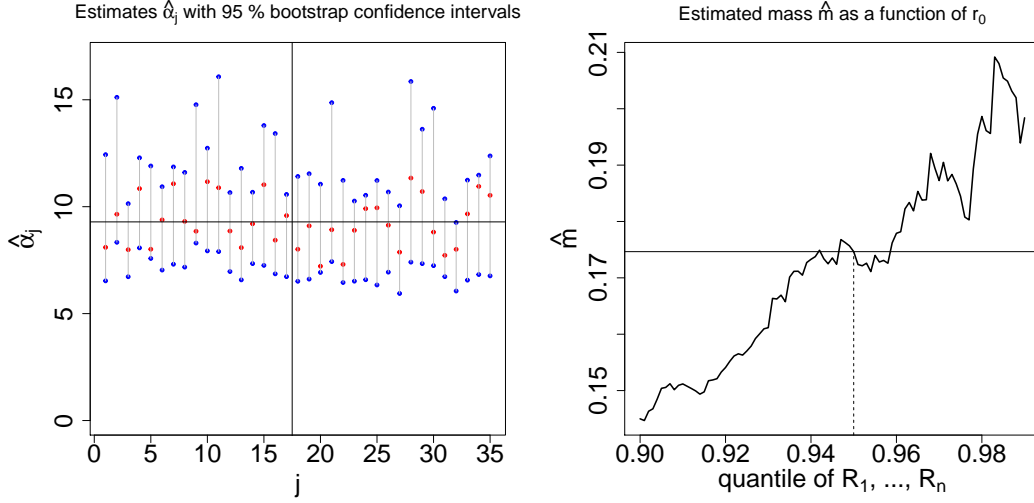


Fig 2: Left: estimates $\hat{\alpha}_j$ with upper and lower 95% confidence limits; the horizontal line represents the estimate $\hat{\alpha}$. Right: estimated mass \hat{m} of the angular measure as a function of r_0 , a high quantile of R_1, \dots, R_n ; the horizontal line represents the estimate for $r_0 = 0.95$.

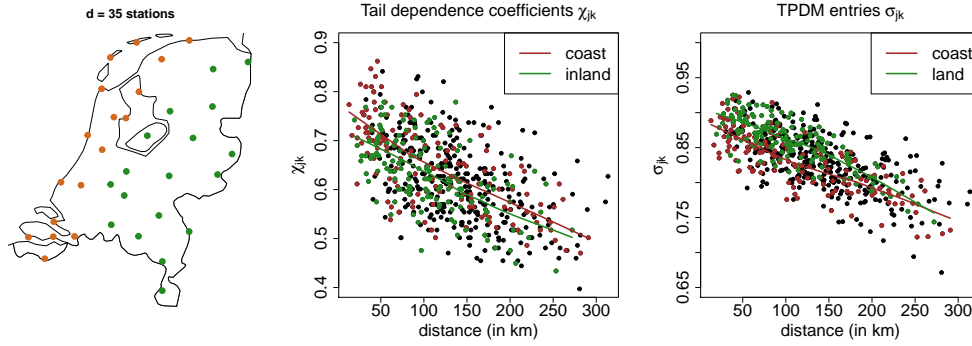


Fig 3: Left: map of the Netherlands with 17 coastal stations in brown and 18 inland stations in green. Middle: empirical coefficients of tail dependence χ_{jk} for all pairs (black), pairs of coastal stations (blue), and pairs of inland stations (red), with loess curves. Right: same but for the TPDM entries σ_{jk} .

winter season), while the last value corresponds to the record wind gusts measured during storm Eunice.

Figure 4 shows boxplots of the estimates based on $\hat{A}_1, \dots, \hat{A}_{200}$, together with estimates based on \tilde{A} and empirical estimates, for the three thresholds (from left to right), on the original scale and the transformed scale. Upper panels represent the analysis using coastal stations only, middle panels are for inland stations only, while lower panels use the full dataset ($d = 35$). While in the univariate and pairwise analysis, no apparent difference was present between coastal and inland stations, when estimating failure probabilities based on the 17- and 18-dimensional datasets, we observe that values for coastal stations are almost five times as high than for inland stations when performing the analysis on the original scale. Smaller differences are found when using the standardized data $\mathbf{X}_1^\#, \dots, \mathbf{X}_n^\#$. The estimates based on the full 35-dimensional dataset are closer to the coastal estimates than to the inland es-

timates. Finally, we see larger discrepancy with the empirical estimates for the 144 km/h threshold, which is due to the estimation uncertainty associated to such a high threshold.

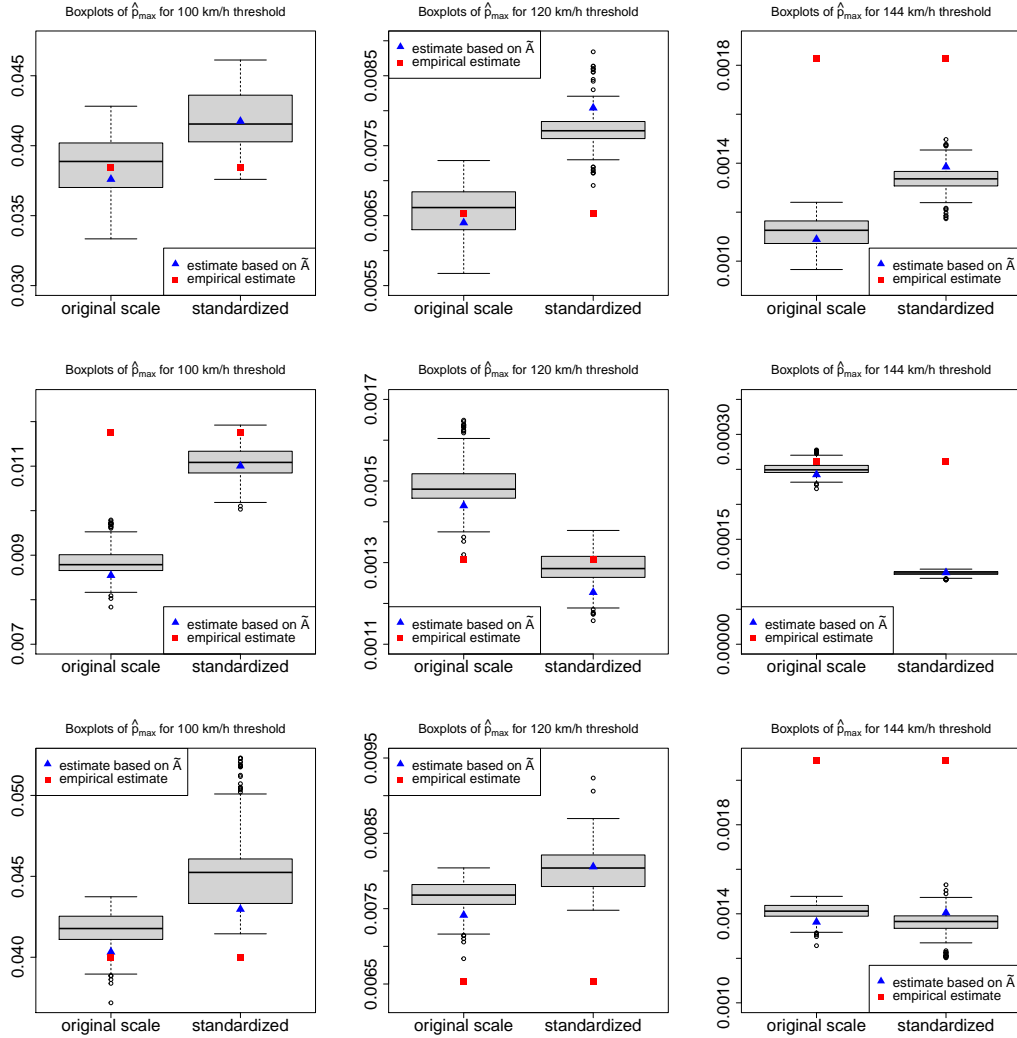


Fig 4: Boxplots of estimates of failure probabilities for the region C_{\max} for the 17 coastal stations (upper panels), the 18 inland stations (middle panels), and all 35 stations combined (lower panels).

5.3. Financial industry portfolios. We focus on the daily negative value-averaged returns of $d = 30$ industry portfolios, downloaded from the Kenneth French Data Library. Data is available for the period January 1970 until December 2019, leading to a sample size $n = 12613$.

We start by estimating the marginal tail indices $\alpha_j = 1/\gamma_j$ using the standard Hill estimator with automated threshold selection (Danielsson et al., 2016). Figure 5 (left) show the estimates, with upper and lower bootstrap confidence limits for a 95% confidence level. Overlapping confidence intervals suggest that the hypothesis of a single index of regular variation

α is not rejected. The marginal estimates are rather similar, and the straight line corresponding to the estimate $\hat{\alpha}$, based on all data combined, is within all confidence intervals. Hence, in the following, we use $\hat{\alpha} = 3.479$.

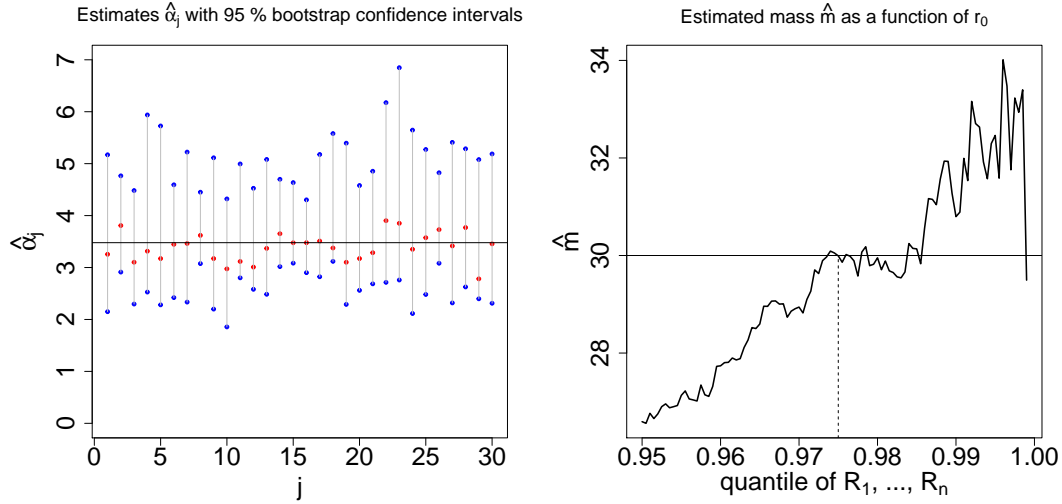


Fig 5: Left: estimates $\hat{\alpha}_j$ with upper and lower 95% confidence limits; the horizontal line represents the estimate $\hat{\alpha}$. Right: estimated mass \hat{m} of the angular measure as a function of r_0 , a high quantile of R_1, \dots, R_n ; the horizontal line represents the estimate for $r_0 = 0.975$.

The next step concerns the choice of r_0 . Figure 5 (right) show estimates of m , the total mass of the angular measure, as a function of r_0 . We continue with r_0 corresponding to the 97.5% quantile and hence $\hat{m} = 29.99$, corresponding to using the 316 largest values.

Finally, we estimate A as described in Section 4.2; in total, we obtain $N = 200$ exact decompositions of $\hat{\Sigma}_{\mathbf{X}}$. Based on \hat{A} and on $\hat{A}_1, \dots, \hat{A}_{200}$, we estimate the following quantities:

1. the probability $p_{\text{sum}} = \mathbb{P}[\mathbf{X} \in C_{(\text{sum})}(\mathbf{v}, x)] = \mathbb{P}[\mathbf{v}^T \mathbf{X} > x]$, where x corresponds to the empirical 0.995 quantile of $(\mathbf{v}^T \mathbf{X}_i)_{i=1, \dots, n}$; in other words, we validate the empirical 99.5% value-at-risk (VaR) associated with a weighted sum of industry portfolio returns.
2. the probability $p_{\text{minsum}} = \mathbb{P}[\mathbf{X} \in C_{f_1}(x)]$ associated with $C_{f_1}(x) = \{\mathbf{y} \in \mathbb{E}_0 : f_1(\mathbf{y}) > x\}$ and

$$f_1(\mathbf{y}) = \min \left(\sum_{j=1}^{10} v_j y_j, \sum_{j=11}^{20} v_j y_j, \sum_{j=21}^{30} v_j y_j \right),$$

where x is the empirical 0.995 quantile of $f_1(\mathbf{X}_1), \dots, f_1(\mathbf{X}_n)$; i.e., we validate the empirical 99.5% VaR associated with the minimum of three weighted sums of industry portfolio returns.

3. the probability $p_{\text{maxsum}} = \mathbb{P}[\mathbf{X} \in C_{f_2}(x)]$ associated with $C_{f_2}(x) = \{\mathbf{y} \in \mathbb{E}_0 : f_2(\mathbf{y}) > x\}$ and

$$f_2(\mathbf{y}) = \max \left(\sum_{j=1}^{10} v_j y_j, \sum_{j=11}^{20} v_j y_j, \sum_{j=21}^{30} v_j y_j \right),$$

where x is the empirical 0.995 quantile of $f_2(\mathbf{X}_1), \dots, f_2(\mathbf{X}_n)$.

For all three failure regions, we compare equal weights, $\mathbf{v} = (1/d, \dots, 1/d)$, and unequal weights, $\mathbf{v} = (0.3, 1.7, 1, 0.3, 1.7, 1, \dots, 0.3, 1.7, 1)$. All probabilities can be calculated analytically based on the estimates $\tilde{A}, \hat{A}_1, \dots, \hat{A}_{200}$; see Section 2.3.

Figure 6 shows boxplots of the estimates based on $\hat{A}_1, \dots, \hat{A}_{200}$ and \tilde{A} . Some deviation is visible with respect to the empirical VaR, which could also be due to the empirical VaR suffering from estimation uncertainty. We note that variability is lowest for the sum-region, and highest for the minsum-region.

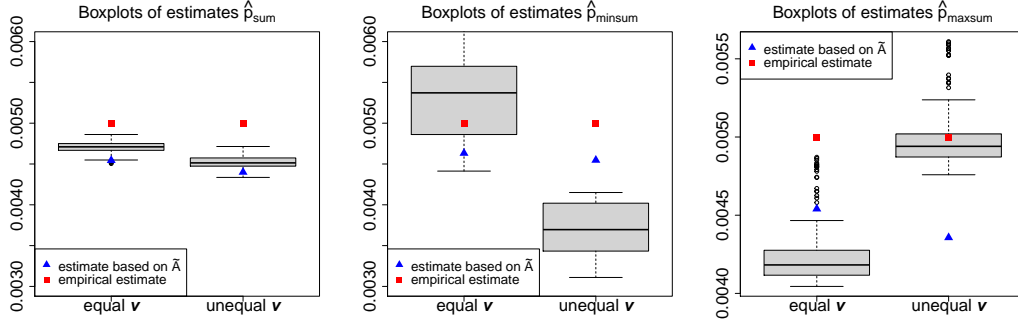


Fig 6: Boxplots of estimates of failure probabilities for the regions $C_{(\text{sum})}, C_{f_1}$, and C_{f_2} for the financial industry portfolios.

6. Discussion. We proposed a general method for the estimation of failure probabilities based on pairwise measures of tail dependence. Our approach is fast and convenient for moderate to high dimensions. When $d \geq 40$, it becomes increasingly hard to find exact decompositions; hence, the (asymptotic) scales of the variables are overestimated, and the approach is appropriate for certain classes of failure regions only.

When summarizing the tail dependence structure through bivariate summary measures, it is natural that some information is lost. However, the ability to obtain repeated decompositions helps in quantifying such uncertainty. Another source of error stems from the estimation of the tail index α and the tail pairwise dependence matrix Σ . Although a multitude of estimators exist for α , estimation of Σ has yet to be investigated further and a better estimator could potentially improve our failure probability estimates.

APPENDIX A: PROOFS

PROOF OF PROPOSITION 2.1. For a vector $\mathbf{X} \in \mathbb{R}^d$, let $m = H_{\mathbf{X}}(\mathbb{S}_{d-1})$ denote the total mass of the angular measure. Then $\tilde{H}_{\mathbf{X}}(\cdot) := m^{-1}H_{\mathbf{X}}(\cdot)$ is a probability measure. Let \mathbf{W} be a random vector that satisfies $\mathbb{P}[\mathbf{W} \in B] = \tilde{H}_{\mathbf{X}}(B)$ for $B \subset \mathbb{S}_{d-1}$. Then $m \mathbb{E} \left[\mathbf{W}^{\alpha/2} (\mathbf{W}^{\alpha/2})^T \right] = \Sigma_{\mathbf{X}}$. Finally, for $\mathbf{y} \in \mathbb{R}^d \setminus \{\mathbf{0}\}$,

$$\mathbf{y}^T \Sigma_{\mathbf{X}} \mathbf{y} = m \mathbb{E} \left[\mathbf{y}^T \mathbf{W}^{\alpha/2} \mathbf{W}^{\alpha/2} \mathbf{y} \right] = m \mathbb{E} \left[\left(\mathbf{y}^T \mathbf{W}^{\alpha/2} \right)^2 \right] \geq 0.$$

□

PROOF OF LEMMA 3.1. We have $\Sigma^{(i)} > 0$ if and only if

$$\sigma_{jk} - \frac{\sigma_{ji}\sigma_{ki}}{\sigma_{ii} \max(D_i, 1)} > 0 \iff \max(D_i, 1) > \frac{\sigma_{ji}\sigma_{ki}}{\sigma_{ii}\sigma_{jk}}, \quad \text{for all } j, k \in \{1, \dots, d\} \setminus \{i\},$$

which is true by definition of D_i . Next, for $\mathbf{x}_{-i} = (x_1, \dots, x_{i-1}, x_{i+1}, \dots, x_d)^T \in \mathbb{R}^{d-1}$ we want to show that $\mathbf{x}_{-i}^T \Sigma^{(i)} \mathbf{x}_{-i} \geq 0$. Let $\mathbf{y} = (y_1, \dots, y_d)^T$ with

$$y_j = \begin{cases} x_j & \text{if } j \in \{1, \dots, d\} \setminus \{i\}; \\ \frac{-\mathbf{x}_{-i}^T \boldsymbol{\sigma}_{-i}}{\sigma_{ii} \max(D_i, 1)} & \text{if } j = i; \end{cases}$$

where $\boldsymbol{\sigma}_{-i} = (\sigma_{1,i}, \dots, \sigma_{i-1,i}, \sigma_{i+1,i}, \dots, \sigma_{d,i})^T$, the i -th column of Σ with the i -th element removed. Because Σ is positive semi-definite, we have $\mathbf{y}^T \Sigma \mathbf{y} \geq 0$. Observing that

$$\begin{aligned} 0 &\leq \mathbf{y}^T \Sigma \mathbf{y} = \mathbf{x}_{-i}^T \Sigma_{(-i,-i)} \mathbf{x}_{-i} + 2y_i (\mathbf{x}_{-i}^T \boldsymbol{\sigma}_{-i}) + y_i^2 \sigma_{ii} \\ &= \mathbf{x}_{-i}^T \Sigma_{(-i,-i)} \mathbf{x}_{-i} - \frac{2(\mathbf{x}_{-i}^T \boldsymbol{\sigma}_{-i})^2}{\sigma_{ii} \max(D_i, 1)} + \frac{(\mathbf{x}_{-i}^T \boldsymbol{\sigma}_{-i})^2}{\sigma_{ii} \max(D_i, 1)^2} \\ &= \mathbf{x}_{-i}^T \Sigma_{(-i,-i)} \mathbf{x}_{-i} + (\mathbf{x}_{-i}^T \boldsymbol{\tau}_{-i})^2 \left(\frac{1}{\max(D_i, 1)} - 2 \right) \\ &\leq \mathbf{x}_{-i}^T \Sigma_{(-i,-i)} \mathbf{x}_{-i} - (\mathbf{x}_{-i}^T \boldsymbol{\tau}_{-i})^2 = \mathbf{x}_{-i}^T \Sigma^{(i)} \mathbf{x}_{-i}, \end{aligned}$$

where the third equality is obtained by observing that $\frac{(\mathbf{x}_{-i}^T \boldsymbol{\sigma}_{-i})^2}{\sigma_{ii} \max(D_i, 1)} = (\mathbf{x}_{-i}^T \boldsymbol{\tau}_{-i})^2$. Hence, we have shown that $\Sigma^{(i)}$ is positive semi-definite. \square

PROOF OF PROPOSITION 3.2. Suppose without loss of generality that $i = 1$. Since \mathbf{Y}_{-1} is a max-linear random vector with TPDM $\Sigma^{(1)}$, for some $q \in \{2, 3, \dots\}$, there exists a coefficient matrix $A_{(-1,-1)} = (a_{jk})_{j=2, \dots, d, k=2, \dots, q} \in \mathbb{R}^{(d-1) \times (q-1)}$ and Fréchet(1, α) random variables Z_2, \dots, Z_q such that

$$\mathbf{Y}_{-1} = A_{(-1,-1)} \times_{\max} (Z_2, \dots, Z_q)^T, \quad \text{and } \Sigma^{(1)} = A_{(-1,-1)}^{\alpha/2} \left(A_{(-1,-1)}^{\alpha/2} \right)^T$$

Then

$$\mathbf{X} = \begin{pmatrix} \tau_{1,1}^{2/\alpha} Z_1 \\ \max(\tau_{2,1}^{2/\alpha} Z_1, Y_2) \\ \vdots \\ \max(\tau_{d,1}^{2/\alpha} Z_1, Y_d) \end{pmatrix} = A \times_{\max} \mathbf{Z}, \quad \text{for } A := \left(\begin{array}{c|ccc} \tau_{1,1}^{2/\alpha} & 0 & \cdots & 0 \\ \tau_{2,1}^{2/\alpha} & & & \\ \vdots & & & \\ \tau_{d,1}^{2/\alpha} & & & \end{array} \middle| A_{(-1,-1)} \right),$$

and $\mathbf{Z} := (Z_1, \dots, Z_q)^T$. We have

$$\Sigma_{\mathbf{X}} = A^{\alpha/2} \left(A^{\alpha/2} \right)^T = \left(\begin{array}{c|ccc} \tau_{1,1}^2 & \tau_{1,1}\tau_{2,1} & \cdots & \tau_{1,1}\tau_{d,1} \\ \tau_{1,1}\tau_{2,1} & & & \\ \vdots & & & \\ \tau_{1,1}\tau_{d,1} & & & \end{array} \middle| \begin{array}{c} \boldsymbol{\tau}_{-1} \boldsymbol{\tau}_{-1}^T + \Sigma^{(1)} \\ \\ \\ \end{array} \right) = \left(\begin{array}{cc} \sigma_{11} \max(D_1, 1) & \sigma_{12} \cdots \sigma_{1d} \\ \sigma_{12} & \sigma_{22} \cdots \sigma_{2d} \\ \vdots & \vdots \ddots \vdots \\ \sigma_{1d} & \sigma_{2d} \cdots \sigma_{dd} \end{array} \right),$$

by the definitions of $\Sigma^{(1)}$, $\boldsymbol{\tau}_1$ and $\boldsymbol{\tau}_{-1}$. Hence, $\Sigma = \Sigma_{\mathbf{X}}$ if $D_1 < 1$ and $\sigma_{11} < \sigma_{\mathbf{X}_{11}}$ if $D_1 > 1$. \square

PROOF OF PROPOSITION 3.4. We prove the Proposition by mathematical induction with respect to d . First, we prove for $d = 2$. Since A is lower triangular, so is the corresponding matrix $A^{\alpha/2}$. For $d = 2$, assume that

$$A^{\alpha/2} = \begin{pmatrix} a_{11} & 0 \\ a_{21} & a_{22} \end{pmatrix}.$$

Then

$$\Sigma_{\mathbf{X}} = \begin{pmatrix} a_{11}^2 & a_{11}a_{21} \\ a_{11}a_{21} & a_{21}^2 + a_{22}^2 \end{pmatrix}.$$

By taking the path $1 \mapsto 2$, we calculate

$$D_1(\Sigma_{\mathbf{X}}) = \frac{(a_{11}a_{21})^2}{a_{11}^2(a_{21}^2 + a_{22}^2)} = \frac{a_{21}^2}{a_{21}^2 + a_{22}^2}.$$

Since $D_1(\Sigma_{\mathbf{X}}) < 1$, we find $\boldsymbol{\tau}_1 = (a_{11}, a_{21})^T$. Correspondingly, we calculate that

$$\Sigma_{\mathbf{X}}^{(-1)} = a_{21}^2 + a_{22}^2 - a_{21}^2 = a_{22}^2.$$

Therefore, the iterative algorithm leads to the matrix

$$A_* = \begin{pmatrix} & 0 \\ \boldsymbol{\tau}_1, & a_{22} \end{pmatrix} = A^{\alpha/2}.$$

The proposition is thus proven for $d = 2$.

Next, assume that the Proposition is valid for $d - 1$ with $d \geq 3$, we show that it is also valid for d . Denote the lower triangular matrix $A^{\alpha/2}$ as

$$A^{\alpha/2} = \begin{pmatrix} a_{11} & 0 & \cdots & 0 \\ a_{21} & a_{22} & \cdots & 0 \\ \vdots & \vdots & \ddots & \vdots \\ a_{n1} & a_{n2} & \cdots & a_{nn} \end{pmatrix} =: \begin{pmatrix} a_{11} & \mathbf{0}^T \\ \mathbf{a}_{-1} & \tilde{\mathbf{A}}^{(-1,-1)} \end{pmatrix},$$

where $\mathbf{0}$ is a $(d - 1)$ -dimensional vector with all elements zero, $\mathbf{a}_{-1} = (a_{21}, \dots, a_{n1})^T$ and $\tilde{\mathbf{A}}^{(-1,-1)}$ is a $(d - 1) \times (d - 1)$ lower-triangular matrix. Then

$$\Sigma_{\mathbf{X}} = \begin{pmatrix} a_{11}^2 & & \\ a_{11}\mathbf{a}_{-1} & \mathbf{a}_{-1}\mathbf{a}_{-1}^T + \tilde{\mathbf{A}}^{(-1,-1)}(\tilde{\mathbf{A}}^{(-1,-1)})^T & \end{pmatrix}.$$

Because $\tilde{\mathbf{A}}^{(-1,-1)}$ contains only non-negative elements, we get $\sigma_{jk} > a_{j1}a_{k1}$ for any $j, k \neq 1$. In addition, $\sigma_{j1} = a_{11}a_{j1}$. Since we consider the path $1 \mapsto 2 \mapsto \dots \mapsto d$, we first calculate D_1 ; for any $j, k \neq 1$,

$$\frac{\sigma_{j1}\sigma_{k1}}{\sigma_{jk}\sigma_{11}} < \frac{a_{11}a_{j1}a_{11}a_{k1}}{a_{j1}a_{k1}a_{11}^2} = 1,$$

which implies that $D_1 < 1$ and thus $\boldsymbol{\tau}_1 = (a_{11}, a_{21}, \dots, a_{d1})^T$ following the algorithm specified in (7). Correspondingly, from (8) we get

$$\begin{aligned} \Sigma_{\mathbf{X}}^{(1)} &= \Sigma_{\mathbf{X}}^{(-1,-1)} - \boldsymbol{\tau}_{-1}\boldsymbol{\tau}_{-1}^T = \mathbf{a}_{-1}\mathbf{a}_{-1}^T + \tilde{\mathbf{A}}^{(-1,-1)}(\tilde{\mathbf{A}}^{(-1,-1)})^T - \mathbf{a}_{-1}\mathbf{a}_{-1}^T \\ &= \tilde{\mathbf{A}}^{(-1,-1)}(\tilde{\mathbf{A}}^{(-1,-1)})^T. \end{aligned}$$

In other words, the $(d - 1) \times (d - 1)$ matrix $\Sigma_{\mathbf{X}}^{(1)}$ is of the form $\tilde{\mathbf{A}}^{(-1,-1)}(\tilde{\mathbf{A}}^{(-1,-1)})^T$ where $\tilde{\mathbf{A}}^{(-1,-1)}$ is a lower-triangular matrix with non-negative elements only. By invoking the assumption that the proposition holds for $d - 1$, we complete the proof of the induction step and conclude that the proposition hold for any positive integer d . \square

APPENDIX B: EXTREME PRECIPITATION IN SWITZERLAND

We focus on daily precipitation amounts in mm for June, July and August for the years 1962–2012 at $d = 44$ weather stations near Zürich, Switzerland, leading to a sample size $n = 4691$. This data was analyzed in [Thibaud and Opitz \(2015\)](#) and [Cooley and Thibaud \(2019\)](#) and found to be stationary, independent in time, and asymptotically dependent in space. Estimates of marginal tail indices tend to vary so that a common index of regular variation α is not justified; we standardize the data to $\mathbf{X}_1^\#, \dots, \mathbf{X}_n^\#$. We take r_0 corresponding to the 95% quantile, yielding 235 “extreme” observations. Finally, we search for estimates of A corresponding to exact decompositions of $\widehat{\Sigma}_{\mathbf{X}}$; a very large number of exact decompositions exists (but with identical paths for the first 14 iterations); we keep $N = 2000$ of them. Based on \widetilde{A} and $\widehat{A}_1, \dots, \widehat{A}_N$, we estimate

1. the probability $p_{(\min)} = \mathbb{P}[\mathbf{X} \in C_{\min}(\mathbf{x})]$, where \mathbf{x} is chosen as the 30 mm threshold for precipitation on the original scale;
2. the probability $p_{(\max)} = \mathbb{P}[\mathbf{X} \in C_{\max}(\mathbf{x})]$, where \mathbf{x} is chosen as the 60 and 80 mm threshold for precipitation on the original scale.

The first probability has also been estimated in [Cooley and Thibaud \(2019\)](#), who found a value of 4.8×10^{-4} . For this region, the N decompositions give the same estimate of $\widehat{p}_{(\min)} = 3.3 \times 10^{-3}$ since only the first column of $\widehat{A}_1, \dots, \widehat{A}_N$ matters. We can compare these to the empirical estimate of 4.3×10^{-4} and the estimate based on \widetilde{A} which gives 1.7×10^{-3} . Figure 7 shows boxplots of the estimates based on $\widehat{A}_1, \dots, \widehat{A}_N$, together with estimates based on \widetilde{A} and empirical estimates for p_{\max} . We see that the estimates based on \widetilde{A} underestimate the probability of a heavy rainfall event.

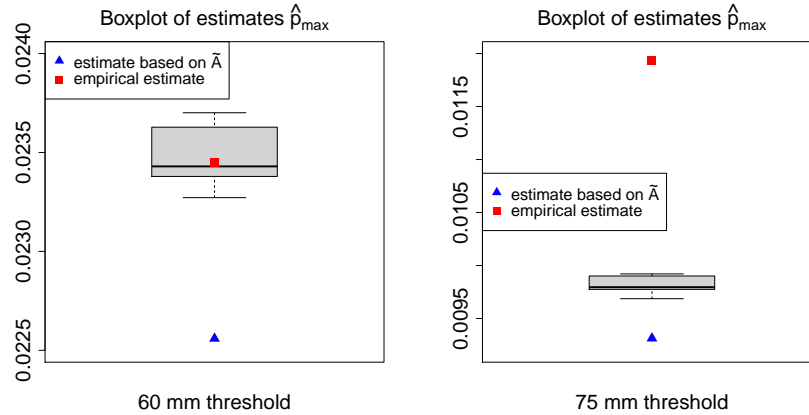


Fig 7: Boxplots of estimates of failure probabilities p_{\max} for the the Swiss precipitation data, for a 60 mm threshold (left) and a 80 mm threshold (right) on the original scale.

Acknowledgments. The authors would like to thank Emeric Thibaud for providing the Swiss rainfall data used in Appendix B.

Funding. Anna Kiriliouk was supported in part by the Fonds de la Recherche Scientifique - FNRS (grant number J.0124.20).

REFERENCES

- BARIOLI, F. and BERMAN, A. (2003). The maximal cp-rank of rank k completely positive matrices. *Linear Algebra and its Applications* **363** 17–33.
- BEIRLANT, J., GOEGEBEUR, Y., SEGERS, J. and TEUGELS, J. (2004). *Statistics of Extremes: Theory and Applications*. Wiley.
- BOŢ, R. I. and NGUYEN, D.-K. (2021). Factorization of completely positive matrices using iterative projected gradient steps. *Numerical Linear Algebra with Applications* **28** e2391.
- CANTY, A. and RIPLEY, B. D. (2020). boot: Bootstrap R (S-Plus) Functions R package version 1.3-25.
- COLES, S., HEFFERNAN, J. and TAWN, J. (1999). Dependence Measures for Extreme Value Analyses. *Extremes* **2** 339–365.
- COOLEY, D. and THIBAUD, E. (2019). Decompositions of dependence for high-dimensional extremes. *Biometrika* **106** 587–604.
- CUI, Q. and ZHANG, Z. (2018). Max-linear competing factor models. *Journal of Business & Economic Statistics* **36** 62–74.
- DANIELSSON, J., ERGUN, L. M., DE HAAN, L. and DE VRIES, C. G. (2016). Tail index estimation: Quantile driven threshold selection. Available at SSRN 2717478.
- DE HAAN, L. and FERREIRA, A. (2006). *Extreme Value Theory: an Introduction*. Springer-Verlag Inc.
- DREES, H. and DE HAAN, L. (2015). Estimating failure probabilities. *Bernoulli* **21** 957–1001.
- EINMAHL, J. H., KIRILIOUK, A. and SEGERS, J. (2018). A continuous updating weighted least squares estimator of tail dependence in high dimensions. *Extremes* **21** 205–233.
- EINMAHL, J. H., FERREIRA, A., DE HAAN, L., NEVES, C. and ZHOU, C. (2022). Spatial dependence and space–time trend in extreme events. *The Annals of Statistics* **50** 30–52.
- FOMICHOV, V. and IVANOV, J. (2020). Detection of groups of concomitant extremes using clustering.
- FOUGERES, A.-L., MERCADIER, C. and NOLAN, J. P. (2013). Dense classes of multivariate extreme value distributions. *Journal of Multivariate Analysis* **116** 109–129.
- GISSIBL, N. and KLÜPPELBERG, C. (2018). Max-linear models on directed acyclic graphs. *Bernoulli* **24** 2693–2720.
- GROETZNER, P. and DÜR, M. (2020). A factorization method for completely positive matrices. *Linear Algebra and its Applications* **591** 1–24.
- HILL, B. M. (1975). A simple general approach to inference about the tail of a distribution. *The Annals of Statistics* 1163–1174.
- JANSSEN, A. and WAN, P. (2020). k -means clustering of extremes. *Electronic Journal of Statistics* **14** 1211–1233.
- KIM, M. and KOKOSZKA, P. (2022). Extremal dependence measure for functional data. *Journal of Multivariate Analysis* **189** 104887.
- KIRILIOUK, A. (2020). Hypothesis testing for tail dependence parameters on the boundary of the parameter space. *Econometrics and Statistics* **16** 121–135.
- KIRILIOUK, A. and NAVEAU, P. (2020). Climate extreme event attribution using multivariate peaks-over-thresholds modeling and counterfactual theory. *The Annals of Applied Statistics* **14** 1342–1358.
- KLÜPPELBERG, C. and KRALI, M. (2021). Estimating an extreme Bayesian network via scalings. *Journal of Multivariate Analysis* **181** 104672.
- LARSSON, M. and RESNICK, S. I. (2012). Extremal dependence measure and extremogram: the regularly varying case. *Extremes* **15** 231–256.
- LENDERINK, G., VAN MEIJGAARD, E. and SELTEN, F. (2009). Intense coastal rainfall in the Netherlands in response to high sea surface temperatures: analysis of the event of August 2006 from the perspective of a changing climate. *Climate dynamics* **32** 19–33.
- MAINIK, G. and EMBRECHTS, P. (2013). Diversification in heavy-tailed portfolios: properties and pitfalls. *Annals of Actuarial Science* **7** 26–45.
- RESNICK, S. I. (2007). *Heavy-tail phenomena: probabilistic and statistical modeling*. Springer Science & Business Media.
- RESNICK, S. and STĂRICĂ, C. (1997). Smoothing the Hill estimator. *Advances in Applied Probability* **29** 271–293.
- SAMORODNITSKY, G. and TAQQU, M. S. (1994). *Stable Non-Gaussian Random Processes: Stochastic Models with Infinite Variance*.
- THIBAUD, E. and OPITZ, T. (2015). Efficient inference and simulation for elliptical Pareto processes. *Biometrika* **102** 855–870.
- VALK, C. D. (2016). Approximation and estimation of very small probabilities of multivariate extreme events. *Extremes* **19** 687–717.